



Published in final edited form as:

J Immunol. 2009 February 15; 182(4): 1912–1918. doi:10.4049/jimmunol.0803777.

A role of IgM antibodies in monosodium urate crystal formation and associated adjuvanticity

Uliana Kanevets^{*}, Karan Sharma^{*}, Karen Dresser[†], and Yan Shi^{*}

^{*}*Immunology Research Group & Department of Microbiology and Infectious Diseases, University of Calgary, Calgary, Alberta T2N 4N1, Canada*

[†]*Department of Pathology, University of Massachusetts Medical School, Worcester, Massachusetts 01655, USA*

Abstract

Uric acid is released from injured cells and can act as an adjuvant signal to the immune system. Uric acid crystals invoke strong inflammatory responses in tissues. While their biological effects are evident and the associated signalling mechanisms are becoming clear, it remains unexplained as to why uric acid precipitates rapidly in vivo, in sharp contrast to the minimal crystallization in vitro. We report here that a group of IgM antibodies are able to bind to these crystals, which is interesting in light that B cell deficient mice do not sense the proinflammatory adjuvant effect of uric acid. The titers of these antibodies increase upon immunization with uric acid crystals. We have produced large quantities of such monoclonal antibodies. The purified IgM antibodies can significantly facilitate uric acid precipitation to form the inflammatory crystals in vitro. Infusion of these antibodies into B cell deficient mice significantly increases the basal level of inflammation in these recipients and restores the host's ability to sense uric acid's adjuvanticity. Therefore, we have identified a factor in determining uric acid precipitation and possibly its ability to function as an endogenous adjuvant. This finding suggests a new mechanism of the pathogenesis of gouty arthritis and uric acid induced immune activation.

Keywords

Antibodies; Danger Signaling; Inflammation; Uric Acid Crystals

Introduction

As the causative agent of gout, uric acid crystal (monosodium urate, MSU) mediated inflammatory response has been a historic topic in medicine (1). It has gained recent interest in immunology since it was found to mediate "danger" signalling (2), and is reportedly involved in many immunological processes (3–5). The MSU crystal mediated pathways are also being intensely investigated (6). However, one conceptual gap remains in contrast to the development concerning this research topic.

Uric acid only activates immune cells following its crystallization, a process similar to its pathogenesis in gout. Normally, uric acid is present in plasma at a concentration of 30–60 ug/ml. However, it has a very limited maximal solubility (70 ug/ml). Beyond 70 ug/ml

Corresponding author: Yan Shi, 4A18 HRIC, 3330 Hospital Dr. NW, University of Calgary, Calgary, Alberta, Canada T2N 4N1, Phone 403-220-2536, Fax 403-270-2772, email: yshi@ucalgary.ca.

The authors declare no conflict of interest.

(hyperuricemia), as seen during large scale cell death in injury or chemotherapy, uric acid is at risk of crystallization. These crystals are the cause of gout, and to the best of our knowledge, form the structure recognized by the immune system as an “endogenous danger” (2). One of the most puzzling subjects in research on gout has been about the mechanisms that govern MSU precipitation. In neutral buffers, soluble uric acid takes 14 days or longer to reach its solubility equilibrium (70 to 100 ug/ml), even from highly supersaturated initial solutions (7–10) (and our own observation). Therefore, there appears to be another important regulator in the blood/tissue that significantly accelerates the rate of MSU crystal formation. Furthermore, as a danger signal, MSU needs to be present at the microgram range to efficiently boost CTL responses (2). Whether there is a mechanism that retains this minuscule quantity of MSU on site and prevents instant diffusion is not known.

Intriguingly, there have been numerous reports that gout specimens isolated from acute phase of the attack were often covered with immunoglobulin like structures (11–18). More specifically, it was reported that injection of MSU crystals into rabbits induced a serum factor that increased the rate of MSU crystal formation (19). Since nucleation is the rate limiting step in crystal formation, it was proposed that this phenomenon was a result of antibodies driving the equilibrium towards crystallization by stabilizing initial nucleating MSU monomers (20). In other words, the initial stacking of monomeric molecules is usually unstable under dispersion forces of the solvent. The binding of antibody is therefore expected to stabilize such a microscopic structure, tilting the balance towards precipitation. However, the concept of crystal binding antibodies and the associated crystallization *in vivo* has remained unproven and research on the issue has stayed dormant since. This issue has become urgent in light of the rapidly growing interest in solid structure mediated immune activation and inflammation (6, 21–24). Conceptually, gouty arthritis and MSU mediated immune activation are similar events. We sought to study whether an underlining *in vivo* mechanism can explain the question of uric acid precipitation in the host.

We report here that mouse serum contains IgM antibodies that bind to MSU crystals via their F(ab)₂ fragment. They also facilitate the precipitation of MSU crystals in uric acid solution. This precipitation effect however, is dependent on an intact IgM structure. Of biological implication, B cell deficient mice cannot sense uric acid as a “danger” or immune regulatory signal, which is readily restored with infusion of monoclonal MSU binding antibodies (UBAs). Our work explains the accelerated uric acid precipitation *in vivo*, aids in our understanding of the mechanisms of “danger”, and provides a testable hypothesis for the pathogenesis of gout.

Materials and Methods

Mice, cells and reagents

All mouse strains were housed at the University of Calgary Animal Resource Centre under protocols approved by the University of Calgary Animal Research Review Committee. muMT mice were purchased from Jackson laboratories. Control IgM antibodies were either purchased from Sigma or produced from similar MSU negative staining mAb hybridomas. CD62L (PE) and CD11b (FITC) antibodies were from Ebioscience. Secondary goat anti mouse IgG + IgM (H+L, 115-095-068), IgM (mu chain, 115-095-020), and F(ab')₂ (115-096-146) antibodies were purchased from Jackson ImmunoResearch. IgM fragmentation kit was from Pierce. SIINFEKL peptide was a gift from Dr. Kenneth Rock of University of Massachusetts Medical School. ⁵¹Cr label was freshly ordered for each experiment from MP Biomedical. C3 complete ELISA kit was purchased from Kamiya Biomedica. All MPO measurement reagents were made in our laboratory from chemicals (all from Sigma). Dendritic cell cultures, cell lines, all other cytokine kits, antibodies, and reagents used in this work have been described previously (25). MSU crystals were produced as previously described (2). Briefly, 4 mg/ml uric acid (Sigma) was dissolved in 0.1 M borate buffer by continuously adjusting the pH to 8.0. The

solution was filtered, the crystals precipitated after 7 days were washed twice with absolute alcohol, once with acetone, and air dried in a tissue culture hood prior to use. The fine structure of these crystals were depicted with electron microscope in a separate report (23). Their immune activation effects in various cell types were not affected in TLR4 or other TLR deficient mice (2,4,23).

Immunization, monoclonal antibody production and HPLC immunoglobulin purification

C57BL/6 (B6) and Balb/c mice were immunized with 1 mg of suspended MSU crystal i. p. in PBS without any adjuvant, and were boosted with the same dose biweekly for 2 months. Antisera were collected at this time point for the FACS analysis. Tail blood (>100 ul) was mixed with 1 ul heparin and spun in a micro centrifuge to remove blood cells. Splenocytes were then harvested and fused with A3A tumor cells using a standard hybridoma protocol (26), with 10^7 tumor partners fused with 4×10^7 splenocytes. Between weeks 2 and 4, 25 ul of cell supernatants from growing hybridomas were used to stain 500 ug of MSU crystals to determine the binding. All clones with moderate to high binding were kept, along with several negative binding IgM controls.

Cytotoxic T cell lysis assay

C57BL/6 or muMT mice were s.c. immunized with 5 ug of OVA coated 1 um diameter latex beads in 100 ul PBS as previously described (2). For those that received the antibody infusion, 500 ug purified antibodies were injected twice via tail vein on the same day prior to the immunization. The immunized mice were rested for 7 days and were then sacrificed, and 5×10^7 splenocytes were stimulated in 10 ml of culture media in the presence of 10^{-7} M of SIINFEKL peptide. 5 days later, 5000^{51}Cr labelled EL4 cells pulsed with 10^{-6} M of SIINFEKL were used as target at the E:T ratios indicated. Unpulsed EL4 cells were used as a background control, which produced negligible reading.

Hybridoma culture, typing, fragmentation and purification

B cell hybridomas were cultured in RPMI with 10% FBS plus 1 mM of HEPES, 25 μM of 2 mercaptoethanol, penicillin/streptomycin antibiotics and HAT (hypoxanthine/ aminopterin/ thymidine) media. As a standard operation, the monoclonal antibody from the supernatant was isolated from 800 ml of the supernatants collected. An equal volume of the supersaturated solution of ammonium sulphate was slowly added to the supernatant to precipitate the antibody. The mixture was centrifuged and only the precipitate was collected and dissolved using 30–50 ml of PBS. This solution was then dialyzed 3 times against PBS overnight. The solution was then analyzed using HPLC. The HPLC analysis was performed with a Shimadzu Prominence system with a CBM-20-A controller, a LC-20AB fluid pump and a SPD-M20A diode array. 500 μL of the antibody solution was injected and analyzed on an Alltech Macrosphere GPC 300A 7u column (Alltech 88181) with an isocratic buffer containing 10 mM phosphate and 120 mM NaCl at pH 7.2. The samples were run at a rate of 1 ml/min over 40 min. The fractions collected were tested for the ability to bind MSU crystals and then the active fractions were collected. This mixture was then further subjected to concentration via centrifugation with a Macrosep 300 K filter (Pall Filtron). The leftover fraction was tested for protein concentration using the BCA protein assay kit (Pierce) and then reconstituted to the final concentration of 2 mg/ml. In some assays, the antibodies were further purified with an UNO 12 column (BioRad) with a BioRad FPLC, with pH 9.6 10 mM ethanolamine as Buffer A and Buffer A plus 1.5 M NaCl as Buffer B, resolved at a rate of 1 ml/min in 25 minutes from 0% Buffer B to 80% Buffer B. IgM fragmentation and the associated analysis were performed with a kit and instructions from Pierce (ImmunoPure IgM Fragmentation Kit)

Flow cytometric analysis of MSU crystals

The flow analysis for MSU crystals was developed in our laboratory by modifying standard cell-based FACS analysis. 100 ul of 1 mg/ml MSU crystal suspension was mixed with 100 ul monoclonal antibody supernatant or 1 ug of purified mAb (or as indicated otherwise) and incubated at room temperature for 20 mins. The crystals were then washed twice with PBS and incubated with 0.5 ul of 1 mg/ml 2nd antibody (FITC) in 100 ul for 10 mins. The crystals were then washed again before FACS analysis. On a BD FACScan (BD Biosciences), MSU crystals showed a smaller size (about 5 – 10 % on a linear scale) on the forward scatter, and higher granularity (one to several folds higher on a linear scale) on the side scatter. Typically, 40,000 to 50,000 total events were collected with Cell Quest, and data were analyzed with Flowjo (Tree Star). Xanthine crystals were produced by first incrementally adding 1 N NaOH into 5 mg/ml xanthine suspension to dissolve the powder at high pH. Once completely dissolved, 1 N HCL was added to bring pH back to 7.0. The crystals thus precipitated were washed in 95% ethanol twice, and once in acetone. The crystals were dried prior to use.

Uric acid precipitation assay

A supersaturated uric acid solution (1 mg/ml) was incubated with various concentrations of a control protein (ovalbumin) and a purified (both by sizing and anion exchange column, about 99% pure by HPLC analysis) antibody, either UBA 11, UBA E6, UBA fragment or a control in 1 ml at the indicated concentrations for 6 hours. The supernatants were removed and wells flushed. 1ml of 0.01 N NaOH solution was added to the wells, and 20 ul of the solution was added to 1 ml of water and read at 292 nm with a spectrophotometer. The conversion to the quantity of uric acid was achieved using a standard curve for UV absorbance from a set of uric acid solutions with known concentrations:

$$Y (\text{uric acid in ug}) = 0.0766 X (\text{UV 292 absorption}) + 0.0298; R^2 \text{ for the curve is } 0.9937.$$

Serum uric acid measurement

Mice were injected i.v. with 500 ug of indicated antibodies or PBS for 3 days, with or without the co-injection of 1 mg of soluble uric acid each day. 24 hours after the last injection, blood from mice was collected into vials with 1 ul of heparin and serum was isolated via centrifugation. 2 μ L of serum was mixed with 198 μ L of Buffer A which contained 10 mM Ethanolamine and 120 mM NaCl adjusted to pH 9.6. This mixture was passed through a nanosep 30 K filter (Pall Filtron), which would allow the uric acid in the sample to pass through but would prevent possible protein contaminants from the sample. 100 μ L of the sample was then injected into the HPLC. Uric acid was resolved on a PolyWAX LP column (The Nest Group) by a gradient of 0– 60% B (10 mM Ethanolamine and 1.12 M NaCl adjusted to pH 9.6) at 0.5 mL/min over 15 min. The HPLC analyses with EZ-start software were done at UV 292 nm. Peak area at 292 nm as a percentage of total area of the sample was used for the calculation of uric acid levels in the serum to minimize run to run or injection volume variability as reported previously (25).

Myeloperoxidase measurement

Myeloperoxidase measurements were performed by a method adapted from Bradley et al. on lung tissue isolated on day 4 from mice injected with antibody and uric acid solution (27). The tissue was homogenized with a 50mM potassium phosphate buffer which contained 0.5 % hexadecyltrimethyl ammonium bromide (HTAB; pH 6.0). The samples were then vortexed and the supernatant was centrifuged for 4 minutes at 5000 rpm. 7 μ L supernatant samples were placed in a 96 well plate and 200 μ L of 0.167 mg/ml o-dianisidine hydrochloride solution containing 0.0005 % (w/v) of hydrogen peroxide was added and the changes in absorbance at

450 nm were measured using a microplate reader. The absorbance measurements were then converted to MPO units. The myeloperoxidase values were generated by multiplying the UV reading by a factor of 0.2528 per a standard protocol. One MPO unit of activity is defined as amount of myeloperoxidase required to degrade 1 micromole of peroxide per minute at 25 ° C.

Complement C3 reading

The blood from mice intravenously injected with antibody and uric acid was isolated using the cardiac puncture technique, heparinised and spun down for 10 minutes at 13,000 rpm to collect serum. The serum samples were then prepared according to the manufacturer's protocol (Mouse Complement C3 ELISA kit, Kamiya Biomedical). The absorbance at 450 nm was measured using a microplate reader. The absorbance was then converted to C3 concentration in mg/ml using a standard curve fitting.

Neutrophil activation

Blood samples were collected from mice injected with UBA E6 or control antibody as in the serum uric acid reading, and were subjected to hemolysis treatment and then stained with CD11b (FITC) and CD62L (PE) antibodies. The samples were then analyzed with flow cytometry.

Statistical analysis

All results were reproduced in at least three independent assays. All error bars are one standard deviation of the test sample groups. Student T test (2 tail) was used to produce the p values shown in the graphs.

Results

1. B cells are required for the uric acid adjuvant effect

We hypothesized that some serum factor, likely antibodies, facilitated and enhanced the immune activation associated with MSU crystals. As such, the proposal predicts that the MSU-mediated immune activation should be substantially decreased in the absence of immunoglobulins in vivo due to the reduced MSU crystal precipitation. We tested the validity of this prediction using muMT (IgH) mice, which lack an important domain of the immunoglobulin mu chain, and therefore lack mature B cells (28). We used a well established protocol of cytolytic T cell (CTL) induction by s.c. immunization of OVA coated latex beads (2,29). Splenocytes from the immunized mice 7 days after the immunization were stimulated with an OVA CD8 epitope peptide (SIINFEKL). 5 days later, the stimulated splenocytes were used in a CTL assay against EL4 cells pulsed with the same peptide. When OVA beads were immunized with supersaturated uric acid or MSU crystal as an adjuvant, the enhancement of CTL responses against OVA was observed in C57BL/6 (B6) mice. In contrast, muMT mice, despite their reported intact T cell responses in other settings (30), failed to show any appreciable CTL activity (Fig 1). This result suggested that the adjuvant effect of uric acid for CTL activation is lost in B cell deficient mice. This outcome is consistent with the possibility that other factors associated with B cells, likely antibodies, played a role in the sensing of uric acid by the host.

2. The presence of MSU binding antibodies

We immunized B6 and Balb/c mice with pre-formed crystals to generate MSU crystal-binding antibodies. The mice were immunized with 1 mg of MSU crystals bi-weekly for two months in the absence of any additional adjuvant. The sera collected from the tail blood from the immunized mice strongly stained MSU crystals as determined by FACS analysis (Fig 2A).

Unimmunized mice also had MSU binding antibodies, albeit at titers somewhere between half to one log lower than the immunized mice (Fig 2A). As a control, the MSU immune sera failed to stain xanthine crystals (Fig 2B). We produced over 300 monoclonal antibodies from the immunized mice by fusing the splenocytes with a tumor partner A3A. About 30% of total clones showed various degrees of staining of the MSU crystals, with 9% showing substantial binding (over a log shift compared with the 2nd antibody alone). Of the mAbs that showed binding, we tested their subtypes by analyzing the supernatants with an antibody subtyping kit, and determined that 85% of them are IgM kappa (Fig 2D), while IgGs and one IgM lambda made up the rest. This indicates that MSU-binding B cells do not frequently undergo antibody class switching. This is a common feature of T-independent B cell responses, as expected for a non-protein antigen (MSU crystals) that would not have a cognate T cell response. The lack of adjuvant in our immunization protocol could also explain the absence of class switch.

Additional controls showed that serum from muMT mice had very low staining of MSU even after a similar immunization schedule, suggesting that the substances bound to MSU are antibodies, in line with Figure 2 that they were detectable by anti immunoglobulin antibodies. (Fig 3A). The low staining of muMT serum of MSU seem to suggest that other serum factors can also interact with the crystal surface, albeit to a much lesser extent than the antibodies. Whether such a low binding had any functional consequence was not further studied in this report. Likewise, the binding of two control antibodies (against mouse and human MHC class I molecules) showed minimal staining as well (Fig 3B). These results and the finding that some similarly produced IgM did not stain the MSU crystals suggest that the binding is likely to be specific. The strong affinity and binding of these antibodies suggests a possible involvement of immunoglobulin-mediated cell activation in the biological functions of MSU crystals, especially in light of the possibility of IgM immune complex formation.

3. UBAs facilitate uric acid crystallization

In the process of generating UBAs, we fortuitously discovered that the presence of these antibodies altered MSU precipitation (detail not shown). To investigate the issue, we incubated supersaturated uric acid (1 mg/ml, pH 8.0) solution with a control protein and purified UBAs (UBA 11 or UBA E6) at different concentrations (Fig 4 and data not shown). After 6 hours (Fig 4) or over night (not shown), the MSU crystals settled at the bottom of the tissue culture plate. After carefully washing the plate to remove residual soluble uric acid, the crystals were resolubilised with 0.01N NaOH, and the amount of precipitation was quantified with UV 292 absorbance. Figure 4 shows that the rate of crystal precipitation was in fact a function of the concentration of UBAs, and was less affected by a control protein (OVA). This result indicates that uric acid precipitation is significantly facilitated by UBAs. This observation seems to suggest that non-specific interaction with other proteins might alter uric acid precipitation to a certain extent, as implicated in an earlier report (9).

One outstanding issue in the UBA mediated MSU precipitation is the mode of contact between the crystal surface and the antibody. To study the binding mechanism between UBAs and the crystal surface, we digested UBAs with an IgM fragmentation kit and produced various immunoglobulin domains. Using the same amount of UBA (E6) as the starting point, the resulting F(ab)₂ completely retained the binding, nearly indistinguishable from the original IgM (Fig 5A). Fc₅u (the Fab deleted pentameric heavy chain) demonstrated no staining at all (Fig 5A). Therefore, MSU binding is F(ab)₂ dependent.

However, the binding itself is not equivalent to the actual crystal precipitation. We mixed a supersaturated uric acid solution (1mg/ml) with 50 ug/ml E6 or its fragments, and incubated the solution for 6 hours. Surprisingly, despite the unabated binding to MSU crystals, the F(ab)₂ fragment completely failed to precipitate the soluble uric acid (Fig 5B). Other control structures, including Fc₅ and a control IgM, MOPC that does not bind MSU, had no effect at

all. It is clear from this assay that antibody affinity is necessary but not sufficient for the uric acid precipitation. The pentameric IgM configuration appears to be a crucial structure for the nucleation and growth of the MSU crystals.

As with other antibodies, one concern was the ability of these antibodies to block MSU crystal interaction with immune cells. We reported early on that MSU crystals are potent stimulators of dendritic cell (DC) activation (2). However, it was possible that MSU mediated activation of DCs might be blocked in the presence of these antibodies. We tested the effect of UBAs on DC activation by co-incubating DCs with MSU and either UBAs or control antibodies as indicated. In the presence of 200 ug/ml MSU crystals, 7 day B6 bone marrow DCs induced by GM-CSF and IL4 were activated to express surface CD86, a characteristic DC activation marker. None of the individual UBA or their combination altered MSU mediated DC activation, similar to that of irrelevant control antibodies (Fig 5C). This data argues that the presence of these antibodies does not interfere with the strong adjuvant activities of MSU crystals, at least with regard to DCs.

4. UBAs restore the sensing of uric acid as an immune adjuvant

The notion that UBA mediates uric acid precipitation predicts that blood uric acid levels should drop following the injection of the antibody. We therefore injected soluble uric acid i.v. followed by an infusion of UBA (see Methods) (25). 3 days later, we collected the sera from tail blood. The sera were passed through a 30 K cut off filter to reduce the UV absorption interference. The pass-through was then injected into a weak anion exchange HPLC column and the uric acid peak absorption at 292 nm was recorded as a percentage of total UV absorption of each run (a method to minimize run-to-run human injection error). Figure 6A shows that in the presence of UBA, the recipient mice demonstrated reduced serum uric acid levels, while a control IgM failed to do so. This result was consistent with our hypothesis that UBAs may indeed cause a phase change of uric acid *in vivo*. As an outcome, the soluble uric acid available in the serum was reduced.

Our work presented above led to the proposal that the presence of UBA determines the precipitation of uric acid and the associated inflammation and adjuvanticity. We first studied if the presence of UBAs alters the overall inflammatory state *in vivo*, as it is expected that the precipitation of MSU crystals will cause certain inflammatory reactions. We measured two common indicators, myeloperoxidase in the lung and total serum complement C3. Myeloperoxidase is a product of neutrophils and its level indicates the accumulation of these cells and tissue inflammation (27). The serum C3 is produced in response to inflammation as well and can be regarded as a general indicator of inflammatory state. (31). Figure 6B (myeloperoxidase measurement) and 6C (complement C3 concentration) show that, following the injection of uric acid and UBA, both of the factors were significantly elevated after 3 days. The control IgM antibodies did not have such an effect. One interesting observation was that in both cases, injection of UBA (E6C7) alone led to higher readings, although the C3 elevation with UBA alone was not statistically significant in comparison to the control (Fig 6C). It is possible that UBAs can cause endogenous uric acid precipitation without the additional infusion. It is also possible that injection of UBA causes stress in the recipient and thus increases the uric acid levels in the animal in response to this sudden infusion of great amounts of antibodies. Because the increases in myeloperoxidase measurements suggested the activation/migration of neutrophils into the tissues, we analyzed their CD62L (L-selectin) level by FACS. Neutrophil activation in inflammation is usually accompanied by the loss of this surface adhesion molecule as the neutrophils migrate into the tissue. UBA injection substantially reduced the expression of CD62L on blood neutrophils while the control IgM appeared to have a smaller but noticeable effect (Fig 6D).

The most critical prediction for our study was that the availability of UBA restores the sensing of uric acid as an adjuvant in B cell deficient mice. We therefore injected UBA and a control IgM i.v. into muMT mice and repeated the assay of Figure 1. If the presence of UBAs enables uric acid precipitation, then the defect in sensing uric acid shown in Figure 1 should be restored. In Figure 7 shows that the addition of UBA significantly elevated the CTL activity to the levels similar to that of the WT mice (Figure 1). Interestingly, the control antibody also occasionally provided an enhancing effect, although to a lesser extent (data not shown). This may suggest that the presence of IgM itself be an important means of local immune response, which may come in addition to uric acid precipitation. Overall, the results were in line with our hypothesis that MSU binding antibodies are a critical factor in determining the uric acid mediated adjuvant effect and inflammation. These UBAs most likely achieve such an effect via their ability to cause MSU crystallization.

Discussion

We report here that IgM antibodies enhance the precipitation of uric acid from solution at relatively low concentrations. Gout has been a recognized disease for centuries (32), and the underlining cause was discovered many years ago (33). So far, many mathematical models have been proposed to delineate the rate of crystallization in relationship with environmental factors, such as the temperature, pH, salt, vibration, and even the material of the container in which the experiments were conducted. (7–10). Yet a formula for predicting the rate of crystal formation remains elusive. The robust onset of gouty arthritis therefore also remains a peculiar event.

Our discovery that uric acid is a danger signal released by dying cells is another example of uric acid's biological effect (2). We reported earlier that a crystallization event is required for this adjuvant effect. We have made substantial progress in understanding how MSU crystals, once formed, interact with dendritic cells by a non-receptor dependent, chemical response with the cellular membrane (23). But no underlining mechanisms with regard to the actual phase transition have been revealed, particularly in vivo. It has long been known that uric acid is one of the principal anti-oxidative systems in mammals, and higher species progressively lose the ability to process this substance, in a likely attempt to gain benefits from its protective functions (34,35). Primates have completely lost any enzymatic activities to process uric acid to allantoin due to a mutational silencing (36,37). This progression permits the increasing likelihood of uric acid accumulation and possible crystallization. Our work suggests that UBAs are an important facilitating factor that results in the actual crystal precipitation.

In gout, it is likely that sustained high uric acid levels lead to macroscopic MSU precipitation. There is some clinical evidence to support our hypothesis. In humans, Ig-coated MSU crystals are found in gout specimens (16–18,38). Electron microscopy revealed that the Fab portion of the antibody is attached to the crystal surface with Fc pointing away from the clusters (14). This is the correct configuration of immune complexes, which frequently triggers activation and inflammatory phagocytosis of accessory cells and APCs. A clear exception is that in humans, IgGs are found to bind MSU (16–18,38), and the role of MSU binding IgM has not been studied. A potential explanation for this observation in humans is that gout is a recurring condition with robust cytokine production. Certain IgM responses may be driven to switch as a result of repeated stimulation and using cytokines as a class switch trigger (39). Another important distinction is that so far we have not been able to directly visualize "gout"-like MSU crystals in mouse tissues, because the intrinsic residual uricase activities prevents the formation of macroscopic crystals. In studying the underlining mechanism of uric acid mediated immune activation, a uricase knock out mouse model would work best; however these mice are not viable due to acute kidney failure (40). To us, it has also been proven futile to visualize the microscopic MSU crystal formation in situ. Prior to our production of UBAs, there had been

no immunological reagents to directly detect MSU crystals in the tissue. The preparation steps for histological or other microscopic analysis, such as Gomori's methenamine-silver method, are incompatible with the microcrystals as they dissolve or dismount quickly in washing steps (our own observation). This report further extends the call for a suitable animal model for this important immunological topic.

The situation may be different in the uric acid immune adjuvant effect. The influx of IgM at the site of tissue stress (41,42) may precipitate as well as anchor the microcrystals in situ of uric acid release. Because the formation of the crystals is at the source of tissue destruction by injury or infection, this would establish a situation where DCs and other antigen presenting cells may come into the close proximity of antigen (self or non-self) and adjuvant (MSU crystals), efficiently enabling immune induction. On another note, it has long been reported that IgM is attracted to the site of injury and is a potent mediator of subsequent tissue damage (42). Whether MSU is one source of the "attraction" remains to be determined.

It is important to note that the identity of the MSU binding antibodies is unknown. We can probably exclude the involvement of B2 B cells due to the lack of cognate protein antigen presentation. B1 and marginal zone B cells differ in the target locations that they protect (43). B1 B cells are mostly located in body cavities while marginal zone B cells tend to engage pathogens that penetrate the blood stream. In human, MSU crystals appear most often in joints. Furthermore, from the substantial amounts of UBAs present in the unimmunized mice, it seems to suggest that B1 cells are the source of UBAs, because B1 antibodies are produced without antigenic stimulation. Signaling-wise, we have recently gained a comprehensive understanding of how MSU crystals can trigger immune cell activation by directly engaging cell surface lipids, particularly cholesterol. This leads to plasma membrane lipid sorting and non-specific aggregation of ITAM containing receptors and down stream activation essentially similar to a phagocytic event (23). However, we have no evidence to rule out immune complex mediated activation. It is known that IgM complexes trigger complement fixation, which is about 1000 fold more efficient than IgG complexes (44). Small peptides released during complement fixation, such as C3a and C5a, are anaphylatoxins (45). Additionally, it has been suggested that there might exist a mouse mu chain Fc receptor (46,47), which would presumably trigger immune activation akin to the better defined FcR mediated inflammatory responses (48,49).

It should be prudently noted that without direct visualization of crystals in vivo, this report lacks an important piece of evidence to support our central hypothesis. The interpretation of our data, particularly the possibility of antibody induced MSU crystal formation in vivo, remains speculative. With advent of new imaging technologies, we remain hopeful that MSU crystal formation in vivo will be directly monitored in due time. Such a methodological development will either substantiate or nullify the main hypothesis of this report, although our proposal that antibodies are a substantial component in uric acid mediated inflammation would still stand.

Our work has added a new angle in the study of urate precipitation and the subsequent inflammatory responses. In recent years, the interest in solid structure-mediated immune activation has grown significantly. However, one question has remained unresolved: where do the endogenous crystals come from? Our work is therefore a timely finding. One interesting fact to consider is that in the original report by Addadi's group, the authors tested several immunization crystals and found that each immune serum produced in rabbit led only to the precipitation of the original immunizing crystal (19,20). This type of "specificity" and the common presence of the crystal binding tissue factors among tested mammals may indicate that MSU specific antibodies are not an oddity. Other crystal depositions in humans could involve antibodies as well, for precipitation and subsequent inflammatory responses.

In summary, our work implicates a role of IgM antibodies in MSU crystal formation and potentially subsequent adjuvanticity/inflammation and provides evidence that it is a biologically relevant event in vivo. It may add a line of investigation on other crystal related arthropathies and pathogenesises, in addition to addressing a lingering question in MSU crystal related immunological research in general.

Acknowledgements

We thank Dr. Kenneth Rock for the facility support; Drs. LianJun Shen, Rachel Gerstein, and Raymond Welsh for reagents and discussion; Drs. Yang Yang and Pere Santamaria for critical review of the manuscript; Shelly Galusha and Melanie Desrosiers for technical assistance; and Ashley D. Mucsi and Winston Pang for editorial assistance.

This project is supported by grants to Y.S. from Alberta Heritage Foundation for Medical Research and Canadian Institutes of Health Research

Abbreviations

MPO, Myeloperoxidase; MSU, Mono Sodium Urate crystals; OVA, Ovalbumin; UBA, Uric acid Binding Antibody.

References

1. Smyth, CJ.; Holers, VM. Gout, Hyperuricemia, and Other Crystal-Associated Arthropathies. New York: Marcel Dekker; 1998.
2. Shi Y, Evans JE, Rock KL. Molecular identification of a danger signal that alerts the immune system to dying cells. *Nature* 2003;425:516–521. [PubMed: 14520412]
3. Behrens MD, Wagner WM, Krco CJ, Erskine CL, Kalli KR, Krempski J, Gad EA, Disis ML, Knutson KL. The endogenous danger signal, crystalline uric acid, signals for enhanced antibody immunity. *Blood* 2008;111:1472–1479. [PubMed: 18029553]
4. Chen CJ, Shi Y, Hearn A, Fitzgerald K, Golenbock D, Reed G, Akira S, Rock KL. MyD88-dependent IL-1 receptor signaling is essential for gouty inflammation stimulated by monosodium urate crystals. *J Clin Invest* 2006;116:2262–2271. [PubMed: 16886064]
5. Hu DE, Moore AM, Thomsen LL, Brindle KM. Uric acid promotes tumor immune rejection. *Cancer Res* 2004;64:5059–5062. [PubMed: 15289304]
6. Martinon F, Petrilli V, Mayor A, Tardivel A, Tschopp J. Gout-associated uric acid crystals activate the NALP3 inflammasome. *Nature* 2006;440:237–241. [PubMed: 16407889]
7. Fiddis RW, Vlachos N, Calvert PD. Studies of urate crystallisation in relation to gout. *Ann Rheum Dis* 1983;42:12–15. [PubMed: 6615025]
8. Iwata H, Nishio S, Yokoyama M, Matsumoto A, Takeuchi M. Solubility of uric acid and supersaturation of monosodium urate: why is uric acid so highly soluble in urine? *J Urol* 1989;142:1095–1098. [PubMed: 2795738]
9. Kippen I, Klinenberg JR, Weinberger A, Wilcox WR. Factors affecting urate solubility in vitro. *Ann Rheum Dis* 1974;33:313–317. [PubMed: 4413418]
10. Loeb JN. The influence of temperature on the solubility of monosodium urate. *Arthritis Rheum* 1972;15:189–192. [PubMed: 5027604]
11. Bardin T, Varghese Cherian P, Schumacher HR. Immunoglobulins on the surface of monosodium urate crystals: an immunoelectron microscopic study. *J Rheumatol* 1984;11:339–341. [PubMed: 6737374]
12. Gordon TP, Ahern MJ, Reid C, Roberts-Thomson PJ. Studies on the interaction of rheumatoid factor with monosodium urate crystals and case report of coexistent tophaceous gout and rheumatoid arthritis. *Ann Rheum Dis* 1985;44:384–389. [PubMed: 4015200]
13. Hashimoto Y, Kohri K, Hayashi Y, Moriyama A, Iguchi M, Asai K, Kato T. Specific detection of kappa light chain in uric acid stones. *Life Sci* 1997;61:249–253. [PubMed: 9217284]
14. Kozin F, McCarty DJ. Molecular orientation of immunoglobulin G adsorbed to microcrystalline monosodium urate monohydrate. *J Lab Clin Med* 1980;95:49–58. [PubMed: 7350240]

15. Landis RC, Yagnik DR, Florey O, Philippidis P, Emons V, Mason JC, Haskard DO. Safe disposal of inflammatory monosodium urate monohydrate crystals by differentiated macrophages. *Arthritis Rheum* 2002;46:3026–3033. [PubMed: 12428246]
16. Nagase M, Baker DG, Schumacher HR Jr. Immunoglobulin G coating on crystals and ceramics enhances polymorphonuclear cell superoxide production: correlation with immunoglobulin G adsorbed. *J Rheumatol* 1989;16:971–976. [PubMed: 2549242]
17. Ortiz-Bravo E, Sieck MS, Schumacher HR Jr. Changes in the proteins coating monosodium urate crystals during active and subsiding inflammation. Immunogold studies of synovial fluid from patients with gout and of fluid obtained using the rat subcutaneous air pouch model. *Arthritis Rheum* 1993;36:1274–1285. [PubMed: 8216421]
18. Terkeltaub R, Tenner AJ, Kozin F, Ginsberg MH. Plasma protein binding by monosodium urate crystals. Analysis by two-dimensional gel electrophoresis. *Arthritis Rheum* 1983;26:775–783. [PubMed: 6305372]
19. Kam M, Perl-Treves D, Caspi D, Addadi L. Antibodies against crystals. *Faseb J* 1992;6:2608–2613. [PubMed: 1592211]
20. Kam M, Perl-Treves D, Sfez R, Addadi L. Specificity in the recognition of crystals by antibodies. *J Mol Recognit* 1994;7:257–264. [PubMed: 7734151]
21. Dostert C, Petrilli V, Van Bruggen R, Steele C, Mossman BT, Tschopp J. Innate immune activation through Nalp3 inflammasome sensing of asbestos and silica. *Science* 2008;320:674–677. [PubMed: 18403674]
22. Eisenbarth SC, Colegio OR, O'Connor W, Sutterwala FS, Flavell RA. Crucial role for the Nalp3 inflammasome in the immunostimulatory properties of aluminium adjuvants. *Nature* 2008;453:1122–1126. [PubMed: 18496530]
23. Ng G, Sharma K, Ward SM, Desrosiers MD, Stephens LA, Schoel WM, Li T, Lowell CA, Ling CC, Amrein MW, Shi Y. Receptor-independent, direct membrane binding leads to cell-surface lipid sorting and Syk kinase activation in dendritic cells. *Immunity* 2008;29:807–818. [PubMed: 18993083]
24. Ogura Y, Sutterwala FS, Flavell RA. The inflammasome: first line of the immune response to cell stress. *Cell* 2006;126:659–662. [PubMed: 16923387]
25. Desrosiers MD, Cembrola KM, Fakir MJ, Stephens LA, Jama FM, Shameli A, Mehal WZ, Santamaria P, Shi Y. Adenosine deamination sustains dendritic cell activation in inflammation. *J Immunol* 2007;179:1884–1892. [PubMed: 17641055]
26. Rock, KL. *Hybridoma Technology in the Biosciences and Medicine: Functional T cell hybridomas*. New York: Plenum Press; 1985.
27. Bradley PP, Priebat DA, Christensen RD, Rothstein G. Measurement of cutaneous inflammation: estimation of neutrophil content with an enzyme marker. *J Invest Dermatol* 1982;78:206–209. [PubMed: 6276474]
28. Kitamura D, Roes J, Kuhn R, Rajewsky K. A B cell-deficient mouse by targeted disruption of the membrane exon of the immunoglobulin mu chain gene. *Nature* 1991;350:423–426. [PubMed: 1901381]
29. Shi Y, Zheng W, Rock KL. Cell injury releases endogenous adjuvants that stimulate cytotoxic T cell responses. *Proc Natl Acad Sci U S A*. 2000
30. Topham DJ, Tripp RA, Hamilton-Easton AM, Sarawar SR, Doherty PC. Quantitative analysis of the influenza virus-specific CD4+ T cell memory in the absence of B cells and Ig. *J Immunol* 1996;157:2947–2952. [PubMed: 8816401]
31. Manthei U, Strunk RC, Giclas PC. Acute local inflammation alters synthesis, distribution, and catabolism of third component of complement (C3) in rabbits. *J Clin Invest* 1984;74:424–433. [PubMed: 6746901]
32. Ruddy, S. *Kelley's Textbook of Rheumatology*. Philadelphia: W.B. Saunders Company; 2001.
33. Storey GD. Alfred Baring Garrod (1819–1907). *Rheumatology* 2001;40:1189–1190. [PubMed: 11600751]
34. Ames BN, Cathcart R, Schwiers E, Hochstein P. Uric acid provides an antioxidant defense in humans against oxidant- and radical-caused aging and cancer: a hypothesis. *Proc Natl Acad Sci U S A* 1981;78:6858–6862. [PubMed: 6947260]

35. Hooper DC, Spitsin S, Kean RB, Champion JM, Dickson GM, Chaudhry I, Koprowski H. Uric acid, a natural scavenger of peroxynitrite, in experimental allergic encephalomyelitis and multiple sclerosis. *Proc Natl Acad Sci U S A* 1998;95:675–680. [PubMed: 9435251]
36. Wu XW, Muzny DM, Lee CC, Caskey CT. Two independent mutational events in the loss of urate oxidase during hominoid evolution. *J Mol Evol* 1992;34:78–84. [PubMed: 1556746]
37. Kissel P, Lamarche M, Royer R. Modification of uricaemia and the excretion of uric acid nitrogen by an enzyme of fungal origin. *Nature* 1968;217:72–74. [PubMed: 5635636]
38. Landis RC, Haskard DO. Pathogenesis of crystal-induced inflammation. *Curr Rheumatol Rep* 2001;3:36–41. [PubMed: 11177769]
39. Zhang K. Accessibility control and machinery of immunoglobulin class switch recombination. *J Leukoc Biol* 2003;73:323–332. [PubMed: 12629145]
40. Wu X, Wakamiya M, Vaishnav S, Geske R, Montgomery C Jr, Jones P, Bradley A, Caskey CT. Hyperuricemia and urate nephropathy in urate oxidase-deficient mice. *Proc Natl Acad Sci U S A* 1994;91:742–746. [PubMed: 8290593]
41. Austen WG Jr, Kobzik L, Carroll MC, Hechtman HB, Moore FD Jr. The role of complement and natural antibody in intestinal ischemia-reperfusion injury. *Int J Immunopathol Pharmacol* 2003;16:1–8. [PubMed: 12578725]
42. Zhang M, Austen WG Jr, Chiu I, Alicot EM, Hung R, Ma M, Verna N, Xu M, Hechtman HB, Moore FD Jr, Carroll MC. Identification of a specific self-reactive IgM antibody that initiates intestinal ischemia/reperfusion injury. *Proc Natl Acad Sci U S A* 2004;101:3886–3891. [PubMed: 14999103]
43. Fagarasan S, Honjo T. T-Independent immune response: new aspects of B cell biology. *Science* 2000;290:89–92. [PubMed: 11021805]
44. Boes M, Esau C, Fischer MB, Schmidt T, Carroll M, Chen J. Enhanced B-1 cell development, but impaired IgG antibody responses in mice deficient in secreted IgM. *J Immunol* 1998;160:4776–4787. [PubMed: 9590224]
45. Hawlisch H, Wills-Karp M, Karp CL, Kohl J. The anaphylatoxins bridge innate and adaptive immune responses in allergic asthma. *Mol Immunol* 2004;41:123–131. [PubMed: 15159057]
46. Sakamoto N, Shibuya K, Shimizu Y, Yotsumoto K, Miyabayashi T, Sakano S, Tsuji T, Nakayama E, Nakauchi H, Shibuya A. A novel Fc receptor for IgA and IgM is expressed on both hematopoietic and non-hematopoietic tissues. *Eur J Immunol* 2001;31:1310–1316. [PubMed: 11465087]
47. Shimizu Y, Honda S, Yotsumoto K, Tahara-Hanaoka S, Eyre HJ, Sutherland GR, Endo Y, Shibuya K, Koyama A, Nakauchi H, Shibuya A. Fc(alpha)/mu receptor is a single gene-family member closely related to polymeric immunoglobulin receptor encoded on Chromosome 1. *Immunogenetics* 2001;53:709–711. [PubMed: 11797105]
48. Aderem A, Underhill DM. Mechanisms of phagocytosis in macrophages. *Annu Rev Immunol* 1999;17:593–623. [PubMed: 10358769]
49. Underhill DM, Ozinsky A. Phagocytosis of microbes: complexity in action. *Annu Rev Immunol* 2002;20:825–852. [PubMed: 11861619]

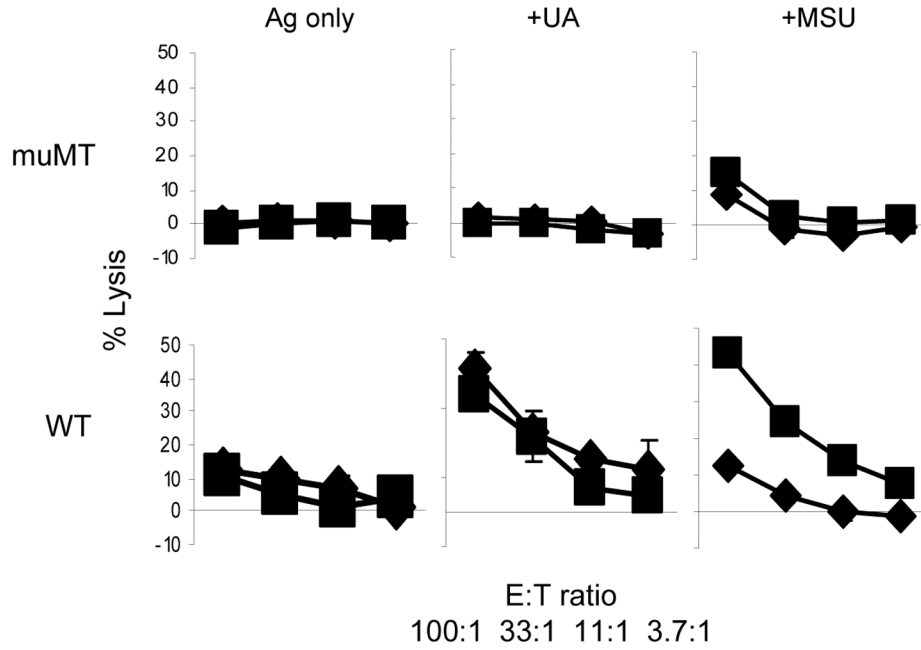


Figure 1. B cell deficient mice do not sense uric acid as an adjuvant

WT or muMT mice were immunized s.c. in the hinder flanks with 5 ug of OVA/latex beads mixed with PBS, 100 ug of MSU crystals or uric acid solution (100 ul total volume). 7 days later, the mice were sacrificed and 50 million splenocytes were prepared and stimulated with the 10^{-10} SIINFEKL peptide. 5 days later, the resulting T cells were counted and the target EL4 (H-2B) cells were labelled with ^{51}Cr and pulsed with the same peptide. A 5 hr CTL assay was performed at the E:T ratio indicated, and as described in the Methods. The two lines in each panel represent two independent mice. The data are representative of 3 independent repeats. Most of error bars (1 standard deviation) were covered by the symbols.

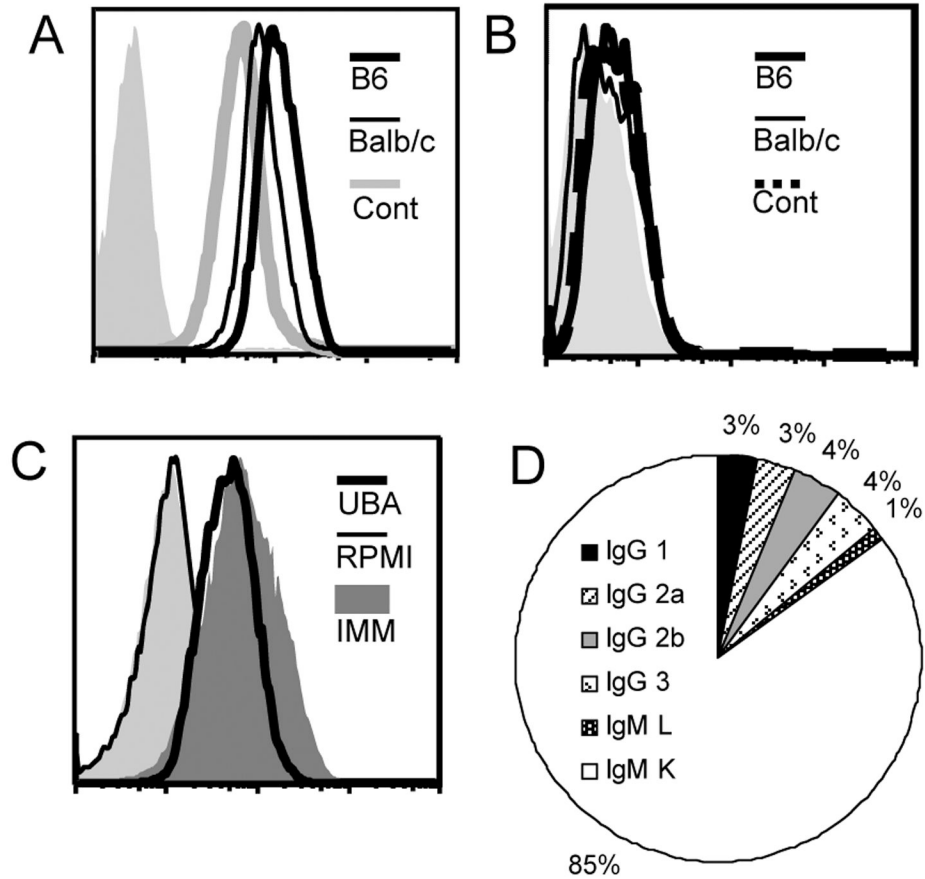


Figure 2. The cloning and analysis of MSU crystal binding antibodies

A. Unimmunized B6 or immunized Balb/c or B6 serum (25 μ l) was used to stain 500 μ g of MSU crystals, followed by a 2nd FITC conjugated antibody recognizing mouse IgG/IgM H +L chains. The FACS analysis is similar to a typical cell-based assay except the crystals are smaller on the forward scatter. The lightly shaded area in this and following assays is 2nd antibody only control. B. Identical to A except xanthine crystals were used in place of MSU. C. Supernatant from a representative high binding UBA (UBA 11, 100 μ l) was used to stain MSU crystals as in A. Imm: MSU immune serum. D. Schematic representation of the frequencies of various immunoglobulin subtypes within MSU binding mAbs.

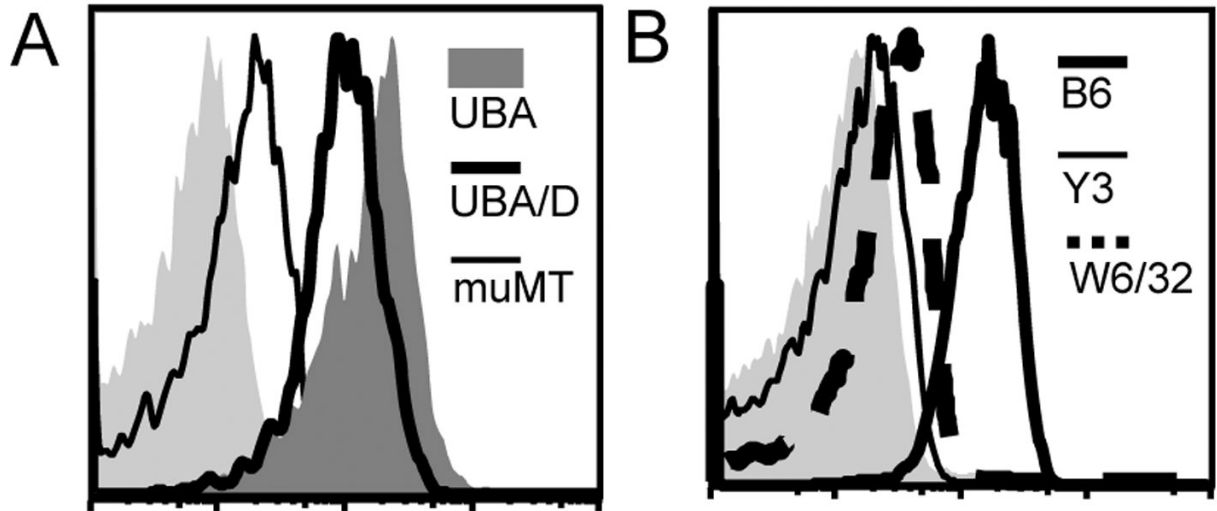


Figure 3. UBAs recognize MSU crystals

A. Similarly immunized muMT serum was compared with an UBA (UBA E6) or a 20 fold dilution of UBA (UBA/D) E6. B. Human (W6/32) or mouse (Y3) MHC class I specific control antibodies do not stain MSU crystals.

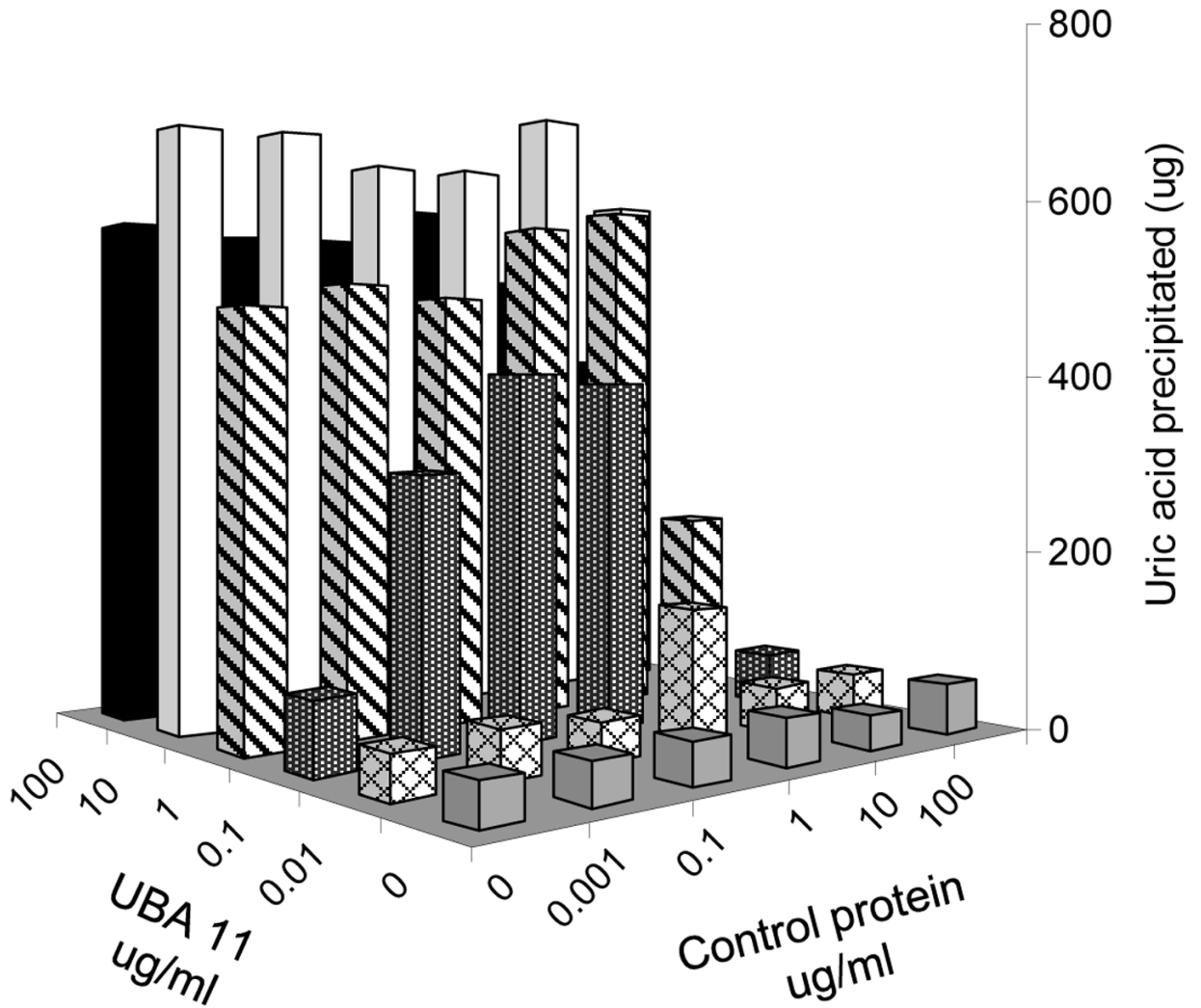


Figure 4. UBAs precipitate soluble uric acid

1 mg/ml uric acid solution in pH 8.0 PBS was incubated with the indicated concentrations of UBA 11 and OVA for 6 hours in 24 well tissue culture plates. The MSU crystals were absorbed at the bottom of the wells (via antibody binding to the plate). The solution was aspirated and the wells were washed with PBS. The deposited MSU crystals were resuspended in 0.01 N NaOH and prepared as described in the methods, and the UV absorption value at 292 nm was determined by a spectrophotometer. The amount of crystal deposition in microgram was converted from a standard UV absorption curve with known uric acid quantities.

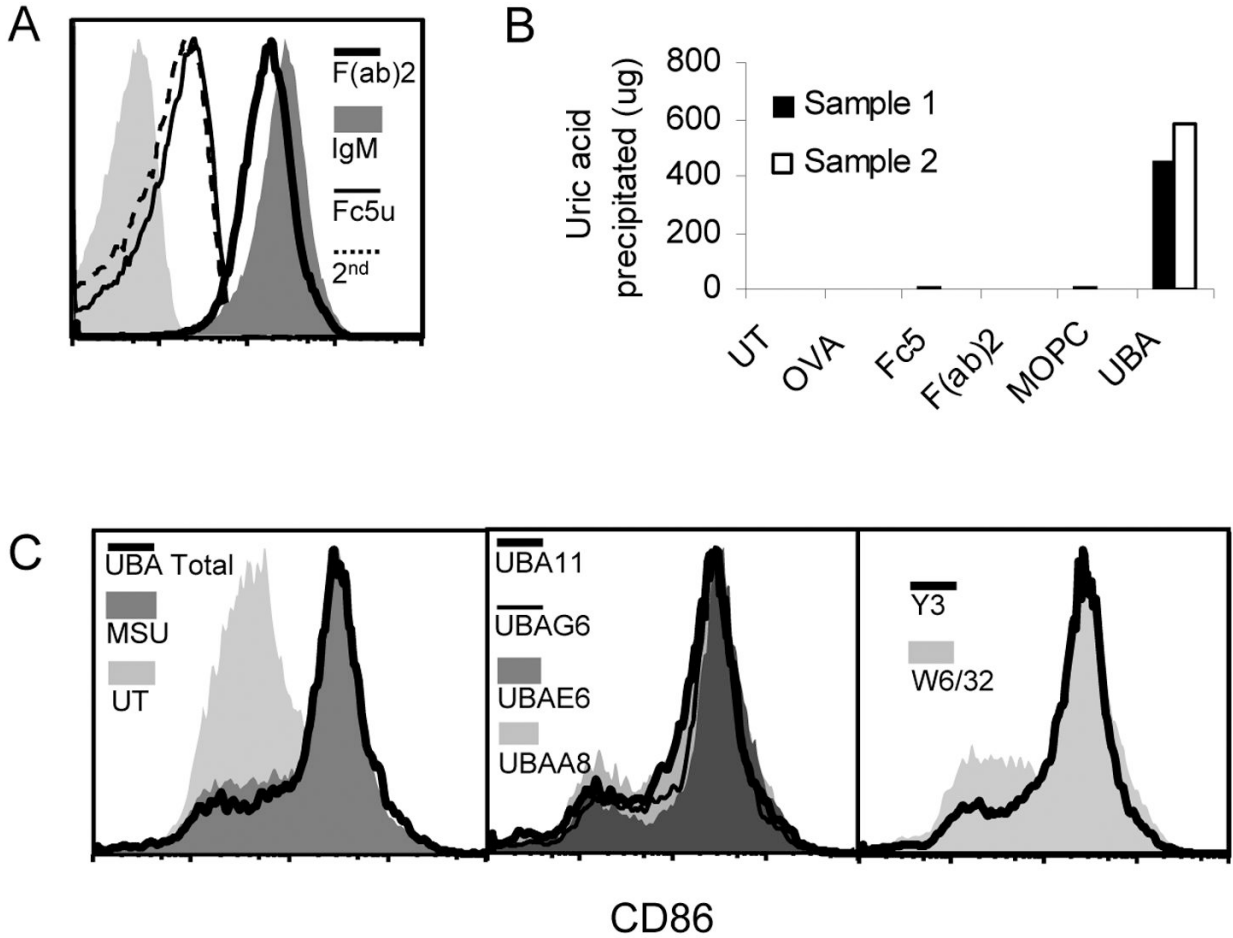


Figure 5. Intact IgM structure is required for MSU crystal precipitation

A. UBA E6 digestion fragments (equal starting amounts) were used to stain MSU crystals. Assays with fragment specific 2nd antibodies produced the same results (data not shown). B. Similar to Figure 4, except that IgM fragments (equal starting amounts) or additional controls (OVA or MOPC control IgM) were used to analyze MSU precipitation. Filled empty bars were two independent replicates. C. Cultured bone marrow GM-CSF/IL-4 DCs were stimulated with MSU and with the addition of indicated mAb supernatants for 6 hours. CD11c positive cells were analyzed for their CD86 expression by FACS.

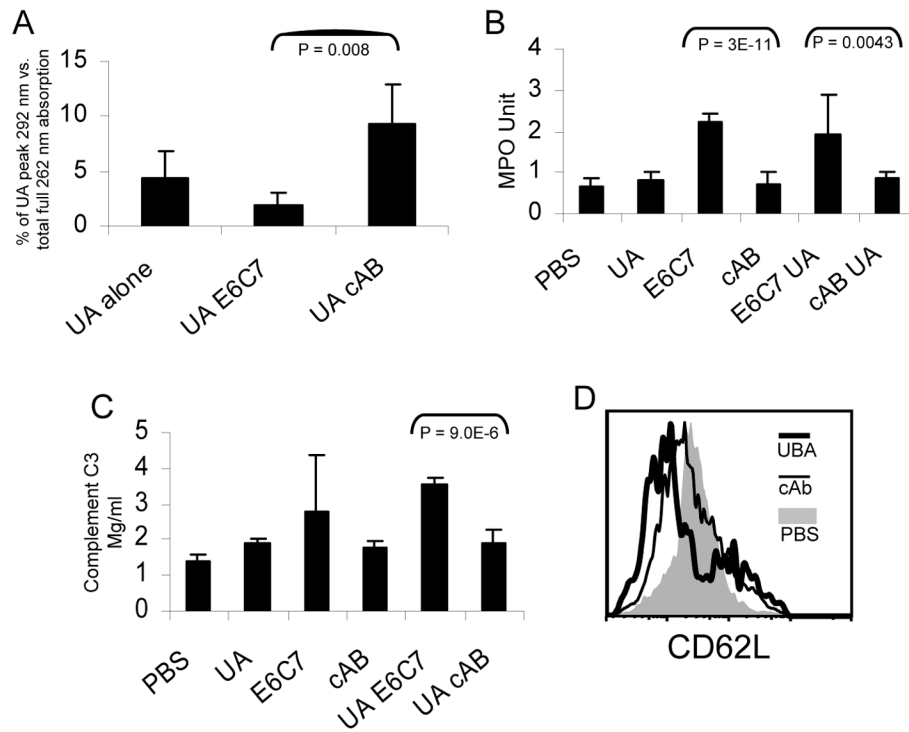


Figure 6. UBAs increase the inflammatory indicators in muMT mice

A. B6 mice were injected i.v. with soluble uric acid (1 mg per day) and indicated antibodies (500 ug per day). UA: uric acid; E6C7: UBA; cAB: control IgM. Serum uric acid levels were analyzed by HPLC as described in Methods. B. The lung tissue from test C57BL/6 mice were homogenized and analyzed as described in the methods section. The myeloperoxidase values were generated by multiplying the UV reading by a factor of 0.2528 per a standard protocol. C. The serum C3 levels in test muMT mice after 3 days of uric acid/antibody infusion were determined using an ELISA kit (see Methods). D. Blood CD11b⁺ cells (neutrophils) were gated and analyzed for their CD62L expression.

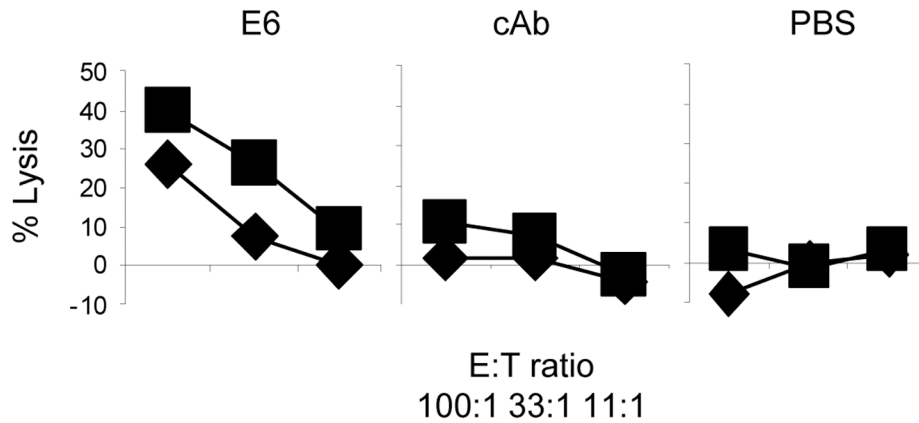


Figure 7. UBAs enable muMT mice to sense uric acid as an endogenous adjuvant

The muMT mice were pre-injected i.v. with 2× of 500 ug purified UBA E6, a control IgM or PBS prior to the immunization s.c. in the hinder flanks with 5 ug of OVA/latex beads admixed with 100 ug of MSU crystals. An assay identical to that in Figure 1 was performed. Control EL4 targets without the peptide pulsing produced no significant reading. The two lines in each panel represent two independent mice. The data are representative of 3 independent experiments.